ChemElectroChem

Research Article
doi.org/10.1002/celc.202400052

Chemistry Europe
European Chemical Societies Publishing

www.chemelectrochem.org

On the Preparation and Spectroelectrochemical Characterization of Certain 2,5-Bis(het)aryl Substituted Thiophenes

Evgenia Dmitrieva,*[a] Jens Barche,[c] Alexey A. Popov,[a] and Horst Hartmann*[b]

In this work, a series of novel 2,5-bis(het)aryl and 2,5-bis-thienyl substituted thiophenes have been synthesized and characterized by ultraviolet-visible-near infrared (UV-Vis-NIR) absorption and fluorescence spectroscopy as well as cyclic voltammetry. From the electron paramagnetic resonance (EPR)/UV-Vis-NIR spectroelectrochemical data, information about the optical and magnetic properties of the charged species of these compounds have been provided. The spin distributions in the electrochemically generated radical ions were estimated experimentally and compared with theoretical data.

Introduction

As is well-known, thiophene is one of the most important building blocks for some types of functional materials, such as for organic field effect transistors (OFETs),[1] organic light emitting diodes (OLEDs),[2] organic solar cells (OSOLs)[3] as well as cell targeting in biomedical applications.[4] Among these compounds, 2,5-bis(het)aryl substituted thiophenes (**6**) occupy a prominent position. They exhibit mostly outstanding electronic properties, such as a highly fluorescence ability,[5] favorable charge transport properties in their solid state[6] and tunable redox potentials,[7] which allow to use these compounds as emitters or as charge transport materials for manufacturing certain types of opto-electronic devices. To obtain a comprehensive description of this class of the compounds in dependence on substituents, we prepared a series of new 2,5-bis(het)aryl substituted thiophenes (**6**) and some of their heterocyclic analogues **12** and **16** by means of an efficient heterocylization procedure. This method starts with simple educts and avoids the use of heavy metals as catalysts for C–C coupling reactions, which are frequently used as alternative method for preparing the target compounds. For studying the electronic properties of the 2,5-bis(het)aryl and 2,5-bis-thienyl substituted thiophenes prepared absorption and emission spectroscopic as well as spectroelectrochemical methods are used. In present work, we have investigated a series of the compounds modified by various peripheral substituents and the backbone to elucidate structure-property relationships in these materials relevant to various redox-related applications. The spectroelectrochemistry is a powerful tool to detect and characterize the charge carriers in the organic semiconductors such as oligo- and polythiophenes.[8] In this study, we used the *in situ* triple method – a unique combination of cyclic voltammetry, EPR and UV-Vis-NIR absorption spectroscopy. The EPR spectroscopy confirms the formation of the electrochemically generated radical ions and helps shed light on the localization of spin, while the UV-Vis-NIR absorption spectroscopy provides the information about their optical properties.

[a] *Dr. E. Dmitrieva, Dr. A. A. Popov*
Leibniz Institut für Festkörper- und Werkstoffforschung (IFW) Dresden
Helmholtzstrasse. 20, 01069, Dresden, Germany
E-mail: e.dmitrieva@ifw-dresden.de

[b] *Prof. Dr. H. Hartmann*
Fakultät für Chemie und Lebensmittelchemie
Technische Universität Dresden
Mommsenstrasse 6, 01062 Dresden, Germany
E-mail: horst.hartmann@tu-dresden.de

[c] *Dr. J. Barche*
Naturwissenschaftliche Fakultät
Martin-Luther-Universität Halle-Wittenberg
and
SAPRI Schkopau GmbH, 06258 Schkopau, Germany
E-mail: jens.barche@freenet.de

Supporting information for this article is available on the WWW under https://doi.org/10.1002/celc.202400052

Results and Discussion

Synthesis

As of now, for the preparation of 2,5-bis(het)aryl substituted thiophenes (**6**) several synthetic methods have been elaborated and described in the literature. Some of those consist in heavy metal catalyzed cross coupling reactions of suited functionalized thiophenes (**1**) with appropriate functionalized arenes (**2**) and/or (**3**) (Scheme 1).[9] Thereby, the aryl-substituted thiophenes **4** or **5** are formed, which can be subsequently transformed by means of similar coupling methods into the target compounds **6**. Although these methods are very meaningful and widely used,[9] other synthetic methods, which generate the essential thiophene moieties by means of a cyclization reaction starting from simple acetophenons (**7**) and benzyl halides (**10**) and avoiding to use heavy metals as catalysts, are also rather valuable.[10]

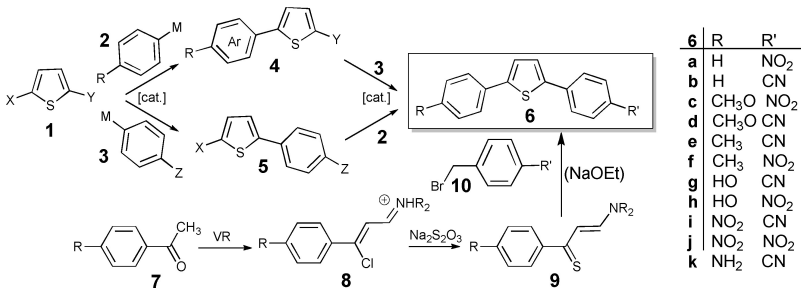

6	R	R'
a	H	NO_2
b	H	CN
c	CH_3O	NO_2
d	CH_3O	CN
e	CH_3	CN
f	CH_3	NO_2
g	HO	CN
h	HO	NO_2
i	NO_2	CN
j	NO_2	NO_2
k	NH_2	CN

Scheme 1. Synthetic routes for preparing the 2,5-bis(het)aryl substituted thiophenes (**6**).

More in detail, one of these methods, which we have used, starts with the 3-aminovinylthioketones (**9**),[11] which can be simply prepared from the acetophenones **7** via the iminium salts **8**,[12] and then allowed to react with benzyl bromides (**10**) under the assistance of sodium ethanolate.[13]

The described heterocyclization procedure for the preparation of the 2,5-bis(het)aryl substituted thiophenes (**6**) have been used in modified manner also for the synthesis of 2-aryl-5-thienyl substituted thiophenes (**12**) and 2,5-bis-thienyl substituted thiophenes (**16**) (Scheme 2). In these cases, the reactions start either with the condensation of the 3-aminovinylthioketones (**9**) with 2-bromomethylthiophenes (**11**) or with the reaction of the thienyl substituted 3-aminovinylthioketones (**15**) with 2-bromomethylthiophenes (**11**). In the first case, the 2-aryl-5-thienyl substituted thiophenes (**12**) and in the second case the 2,5-bis-thienyl substituted thiophenes (**16**) are formed, respectively. The necessary thienyl substituted 3-aminovinylthioketones (**15**) are prepared accordingly to the synthesis of the 3-aminovinylthioketones (**9**) by reaction of 2-actylthiophenes (**13**) with the Vilsmeier reagent (VR), followed by a subsequent reaction of the formed 3-chloropropeniminium salts (**14**) with Na_2S,[14] whereas the necessary 2-bromomethylthiophenes (**11**) are prepared by reaction of the appropriate 2-methylthiophenes with *N*-bromosuccinimide.[15] Table S1 informs on the compounds prepared by means of the heterocyclization methods outlined. As can be seen, the 2,5-bis(het)aryl substituted thiophenes are available in moderate to good yields.

Spectroscopic properties

All the prepared compounds **6**, **12** and **16** are colorless or pale-yellow colored solids that exhibit intense absorption in the UV or short-wavelength visible region as well as a substituent-depending florescence in the visible region. The spectroscopic properties of the 2,5-bis(het)aryl substituted thiophenes are documented by absorption and emission spectroscopy and are represented in Table 1. The absorption and emission spectra are recoded in dioxane. The emission band of the compounds studied ranges from 410 nm for **6b** to 536 nm for **6j**. The Stokes shift ranges between 39 nm for compound **16b** and 191 nm for compound **12c**.

Electrochemical properties

2,5-bis(het)aryl substituted thiophenes were studied by cyclic voltammetry. All these compounds can be electrochemically oxidized and reduced (Figure 1 and S1). The redox potentials of the compounds are displayed in Table 1.

Here, and in the following section, we consider the cyano-substituted derivatives containing the backbone PhThPh and various substituents R in detail to study the influence of the substituent on the electrochemical properties of the compounds. Also, the compounds containing the same substituents (R=CH_3 and R'=CN) but different backbones (PhThPh vs PhThTh vs ThThTh) were compared.

The oxidation potentials of the cyano-substituted derivatives decrease, as expected, with the increase of the electron donating ability of the substituents, namely, from 1.16 V for **6b** (R=H) to 0.36 V for **6k** (R=NH_2). However, the electron deficient nitro-substituted compound **6i** does not show an oxidation in the inert potential window of the electrolyte solution. The most of compounds show an irreversible oxidation with an exception of **6d** containing CH_3O group. As shown for the various molecules containing thiophene[16] or phenyl[17] rings, the irreversible oxidation process is caused by the C–C coupling reactions between a positively charged molecule and its

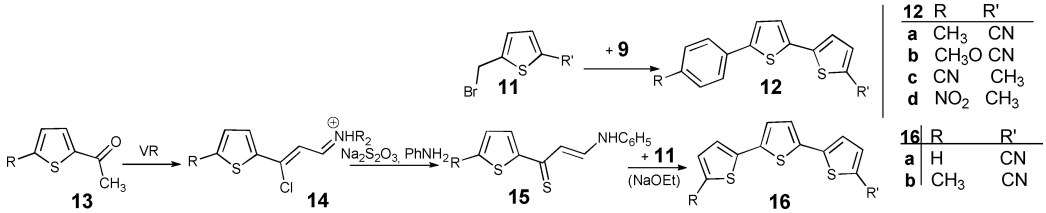

12	R	R'
a	CH_3	CN
b	CH_3O	CN
c	CN	CH_3
d	NO_2	CH_3

16	R	R'
a	H	CN
b	CH_3	CN

Scheme 2. Synthetic routes for preparing the 2-aryl-5-thienyl substituted thiophenes (**12**) and 2,5-bis-thienyl substituted thiophenes (**16**).

Table 1. Spectroscopic and electrochemical data of 2,5-bis(het)aryl substituted thiophenes studied.

compound	R	R′	λ_{abs} [nm][a]	log ε	λ_{fluor}[nm][b]	Δλ [nm] ([eV])	E_{red} [V][c]	E_{ox} [V][d]
6a	H	NO_2	379	4.47	468	89 (0.62)	−1.50	1.05*
6b	H	CN	346	4.72	410	64 (0.56)	−2.20	1.16*
6c	CH_3O	NO_2	379	3.66	527	149 (0.92)		
6d	CH_3O	CN	356	4.23	431	75 (0.61)	−2.21	0.80
6e	CH_3	CN	351	4.00	416	65 (0.55)	−2.20	1.03*
6f	CH_3	NO_2	392	3.92	496	104 (0.66)		
6g	HO	CN	359	4.26	433	74 (0.59)	−2.41	0.81*
6h	HO	NO_2	377	4.13	535	158 (0.97)		
6i	NO_2	CN	396	3.76	475	79 (0.52)	−1.46/−1.96	–
6j	NO_2	NO_2	368	4.04	536	168 (1.06)	−1.64	–
6k	NH_2	CN	379	4.17	475	96 (0.66)	−2.29	0.36*
12a	CH_3	CN	366	4.16	439	73 (0.56)	−2.24	0.93*
12b	CH_3O	CN	374	3.75	450	76 (0.56)	−2.12	0.84
12c	CN	CH_3	303	3.77	494	191 (1.58)	−2.37*	–
12d	NO_2	CH_3	397	4.07	533	136 (0.80)	−1.53	0.76*
16a	H	CN	373	4.30	456	83 (0.61)	−2.30	1.01*
16b	CH_3	CN	383	4.31	422	39 (0.30)	−2.08	0.78

[a,b] The spectra were measured in dioxane. [c,d] Half-wave potential ($E_{1/2}^0$) – for reversible process, peak potential (E_p) – for irreversible process marked by asterisk (0.1 M *n*-Bu_4NPF_6 in acetonitrile).

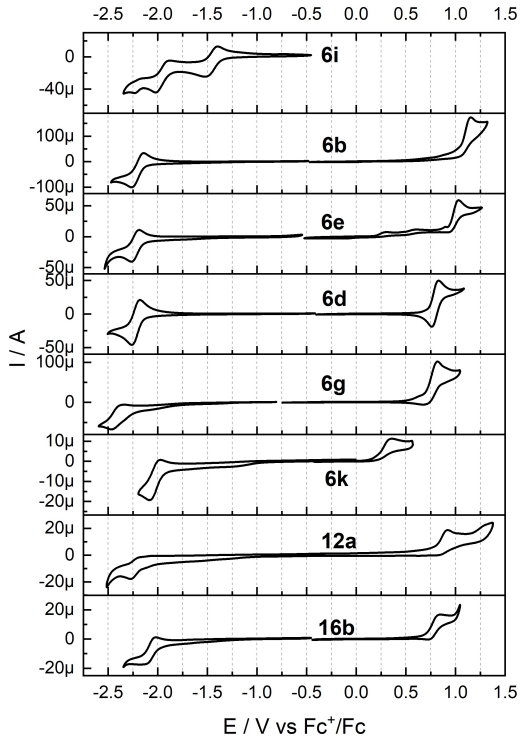

Figure 1. Cyclic voltammograms of cyano-substituted thiophenes measured on Pt in acetonitrile (0.1 M *n*-Bu_4NPF_6) at the scan rate of 0.1 V/s.

precursor. In **6b** (R=H) and **6k** (R=NH_2), the oxidative coupling is realized via the free para-position or via involving the amino group, respectively. In the case of **6g** (R=OH), the phenol radical cation is unstable and immediately undergoes follow-up chemical reaction such as deprotonation and dimerization.[18] Moreover, the previous studies have shown that the C–C coupling in oligothiophenes is also possible through the activation of the β-position and formation of a σ-bond between two thiophene rings.[19] Such coupling was observed for the electron deficient oligothiophenes. This could explain why a stable radical cation is only formed in the case of **6d** containing strong electron donating substituent. The oxidation potential of conjugated oligomers decreases with increasing the effective conjugation length (e.g. by increasing the number of aromatic units) as well as by increasing the electron density in the molecule (by introduction of the electron-donating groups into the molecular structure).[20]

By replacing of the phenylene rings with thiophene moieties, the oxidation potential decreases with increasing of the number of the thiophene rings in the molecular structure (1.03, 0.93 and 0.78 V for the row **6e–12a–16b**). The electronic conjugation in three-ring phenylene–thiophene oligomers is higher for the ThThTh molecule due to increased ring-ring planarity (ring-ring dihedral angle decreases from PhThPh to ThThTh).[21] The coplanarity of the molecule promotes strong electronic delocalization increasing the stability of the radical cations. In contrast to **6e**, the compound **16b** exhibits a reversible oxidation.

All cyano-substituted derivatives show a reversible reduction process in the potential range from −2.2 to −2.4 V vs Fc^+/Fc. In contrast, **6i** containing the electron withdrawing nitro group exhibits two reduction peaks at significant lower negative potentials of −1.46 and −1.96 V.

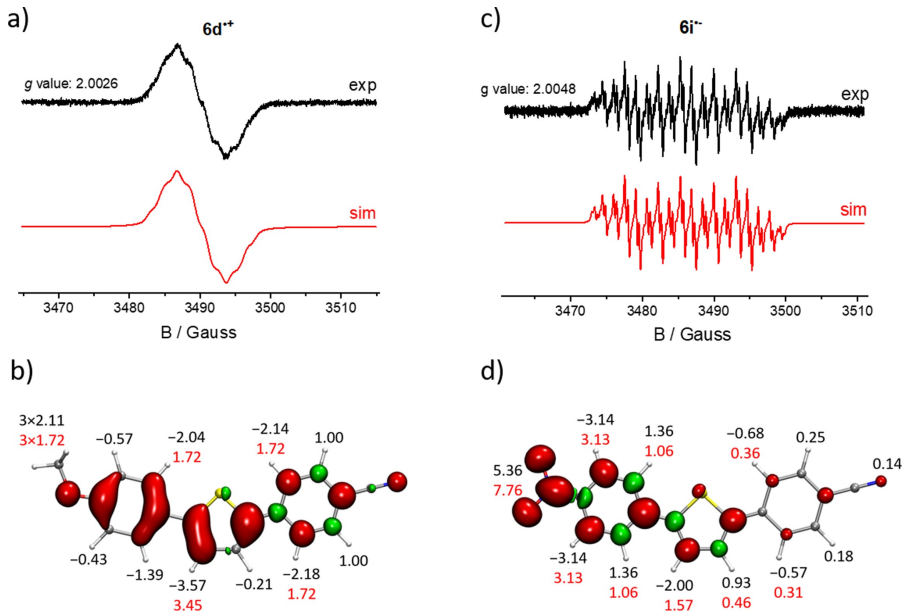

Figure 2. Experimental and simulated EPR spectrum of the radical cation **6d**$^{\bullet+}$ (a) and radical anion **6i**$^{\bullet-}$(c). Spin density distribution in **6d**$^{\bullet+}$ (b) and **6i**$^{\bullet-}$ (d). The numbers are hyperfine coupling constants (in Gauss) determined from the DFT calculations (black) and from the fit to the experimental spectrum (red).

Spectroelectrochemical properties

To gain insight about the charged structures of the 2,5-bis(het)aryl substituted thiophenes (R–PhThPh–R′), the EPR/UV-Vis-NIR spectroelectrochemical study has been performed on selected cyano-substituted derivatives. The compound **6d** with R=CH_3O shows a one-electron reversible oxidation and reduction in the available potential window of electrolyte solution indicating the formation of a stable radical cation **6d**$^{\bullet+}$ and anion **6d**$^{\bullet-}$, respectively. Upon oxidation of **6d**, the EPR spectra show a signal with a *g* value of 2.0026 and a hyperfine structure. The experimental and simulated spectrum are shown in Figure 2a. In radical cation **6d**$^{\bullet+}$, the hyperfine splitting pattern is mostly caused by the interaction of the unpaired electron spin with several protons ($a(^1H) = 3.45$ and 1.72 Gauss) in the phenylene and thiophene rings as well as methoxy group. Smaller hyperfine coupling constants cannot be resolved due to the line width of ca. 1 Gauss. EPR spectroscopic data show that the spin density in the radical cation is delocalized over the whole molecule with small contribution of the cyano group. The spin density distribution in the radical cation derived from the DFT calculations is displayed in Figure 2b and S2 and supports the experimental data. The EPR analysis of the radical anion **6d**$^{\bullet-}$ was not possible due to the overlapping with signal from the electrolyte solution generated at high negative potential.

In contrast to **6d**, the first reduction of **6i** containing nitro group occurs at a relatively low negative potential and gives rise to the formation of the corresponding radical anion **6i**$^{\bullet-}$ which can be studied by EPR spectroscopy. The EPR spectrum shows a signal with a *g* value of 2.0048 and well-resolved hyperfine structure. The experimental and calculated EPR spectrum are in excellent agreement (Figure 2c). The largest coupling constant is due to the one nitrogen nucleus ($a(^{14}N) = 7.76$ Gauss) in the NO_2 group, the other ones are originated from the backbone protons. The EPR measurements and DFT calculations indicate that the spin density in the radical anion is strongly shifted to the region of the nitro group and mostly localized on it and neighboring phenylene ring as plotted in Figure 2d.

Figure 3 displays the UV-Vis-NIR spectra measured during the reduction of **6d**, **6e**, **6b** and **6i** containing CH_3O, CH_3, H and NO_2 group, respectively. The radical anions show an absorption in the visible region of 490–550 nm and a broad absorption in the near infrared region of 800–1050 nm. The bands in the optical spectra of **6d**$^{\bullet-}$ and **6i**$^{\bullet-}$ (with CH_3O and NO_2 group, respectively) are blue shifted compared to **6b**$^{\bullet-}$ with R=H. The spectra of **6b**$^{\bullet-}$ and **6e**$^{\bullet-}$ (R=CH_3) are almost identical. Because of the reversible redox behavior of **6d**, the spectral features of the radical cation and anion can be compared. The UV-Vis-NIR spectrum of the radical cation **6d**$^{\bullet+}$ demonstrates two prominent bands at 515 and 838 nm, while the radical anion **6d**$^{\bullet-}$ exhibits significantly red shifted absorption bands (533 and 888 nm) (Figure S3). The UV-Vis-NIR data demonstrate that the electrochromic properties of the materials under study can be easily fine-tuned by the introduction of the peripheral substituents into the structure.

The compound **16b**, as a representative example of the 2,5-bis-thienyl substituted thiophenes (R–ThThTh–R′), has been also studied by spectroelectrochemistry. Due to its reversible redox behavior with a relative low oxidation potential and a higher reduction potential it was possible to study the both EPR and UV-Vis-NIR spectroscopic features of the negatively and positively charged species. The UV-Vis-NIR absorption bands of the radical anion of **16b**$^{\bullet-}$ (598 and 1038 nm) are remarkably red shifted in comparison to that of the corresponding radical

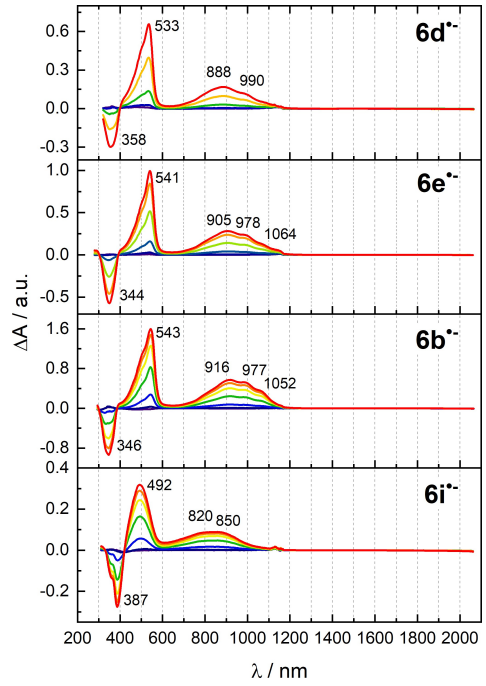

Figure 3. *In situ* UV-Vis-NIR spectra measured during the reduction of **6d, 6e, 6b** and **6i**. The negative potential values increase from blue to red. Each spectrum was collected relative to that of the uncharged compound. Electrolyte: 0.1 M *n*-Bu_4NPF_6 in acetonitrile.

cation **16b**$^{\bullet+}$ (542 and 864 nm) (Figure 4a,b). It should be also mentioned that the optical spectrum of the radical anion **16b**$^{\bullet-}$ is red shifted relative to that of its 2,5-bis(het)aryl substituted analogue **6e**$^{\bullet-}$ containing the PhThPh backbone (Figure 3 and 4b). The extension in π-conjugation length results in the decreasing the optical band gap and, thus, the wavelengths tend to be shifted toward the long wavelength region (red shift). The increased backbone planarity from PhThPh to ThThTh results in extended conjugation lengths, which is manifested by a red shift.[21] The information about the spin density distribution in radical anion and cation of **16b** was extracted from the EPR spectroscopy. The EPR spectra of the radical cation and anion showing different pattern are displayed in Figure 4c,d. The *g* values of **16b**$^{\bullet+}$ (2.0024) and **16b**$^{\bullet-}$ (2.0048) are also distinguished significantly. The DFT calculations have revealed that the spin density in the radical cation is distributed on the hydrocarbon backbone with the small contribution of nitrogen atom in the cyano group (Figure 4e,f). In the case of radical anion, a higher portion of sulfur atoms is involved in the spin density distribution. The extension in the spin density distribution in **16b**$^{\bullet-}$ can explain the remarkable red shift of its absorption bands in the UV-Vis-NIR spectra. The obtained data coincides with that reported earlier for the symmetric α,ω-dicyano substituted quaterthiophene[19] pointing to the similar pathway of the charge distribution along the oligothiophene chain. It has been shown that the optical properties of the charged molecules can be also tuned by modification of the backbone molecule through the introduction of the thiophene rings into molecular structure. Electrochromic properties of the substituted thiophenes studied in this work can be varied in the visible spectral range of 490–600 nm.

Experimental Section

Synthesis

Experimental details for the preparation of the 2,5-bis(het)aryl and 2,5-bis-thienyl substituted thiophenes **6**, **12** and **16** and their precursors are documented in Supporting Information.

Spectroscopic measurements

UV-Vis absorption spectroscopy was conducted on a Shimadzu 3100 spectrophotometer. The fluorescence spectra were recorded on a Perkin Elmer Lambda 900 spectrometer using an excitation wavelength of 391 nm. The UV-Vis absorption and emission spectra were measured in dioxane solution at ambient temperature.

Electrochemical measurements

Cyclic voltammetry (CV) was carried out on a PARSTAT4000 potentiostat (Princeton Applied Research, Ametek, Germany) in a three-electrode cell in degassed dry acetonitrile solution containing 0.1 M of tetra-*n*-butylammonium hexafluorophosphate (*n*-Bu_4NPF_6) as a supporting electrolyte. A Pt disk, AgCl-coated silver wire, and Pt sheet electrode were used as the working electrode, the reference electrode, and the counter electrode, respectively. The Pt electrodes were polished with 1 μm diamond and 0.3 μm alumina suspension, sonicated, rinsed in double distilled water, and then air-dried. All potentials are given versus Fc^+/Fc redox couple as an internal standard. The electrochemical measurements were performed under inert (nitrogen) atmosphere and at ambient temperature.

EPR/UV-Vis-NIR spectroelectrochemical measurements

The EPR/UV-Vis-NIR spectroelectrochemical technique has been described earlier.[22] For EPR measurements, EMX X-band CW spectrometer (Bruker BioSpin, Germany) at 100 kHz modulation was used. The spectra were recorded in an optical EPR cavity (Bruker, Germany) allowing the connection of two optical wave guides to measure the electronic absorption spectra *in situ* in transmission mode and the EPR spectra simultaneously. An NMR teslameter (Bruker, Germany) was used for precise *g* value determination. The UV-Vis-NIR spectra were measured using the Avantes spectrometer AvaSpec-2048×14-USB2 with the CCD detector and AvaSpec-NIR256-2.2 with the InGaAs detector (Avantes, The Netherlands). A light source Avantes Avalight-DH-S-BAL was used. Both, the EPR spectrometer and the UV-Vis-NIR spectrometer are linked to a HEKA potentiostat PG 390 which triggers both spectrometers. At ambient temperature, the EPR and UV-Vis-NIR spectra were collected at a continuous potential scan rate (ca. 5 mV/s). Each UV-Vis-NIR spectrum was collected relative to that of the neutral (uncharged) compound. In spectroelectrochemical experiments, an EPR flat cell with a laminated gold μ-mesh (Goodfellow, UK) as working electrode, an AgCl-coated silver wire as reference electrode, and a platinum wire as counter electrode was used. The cell assembling was done under an inert (nitrogen) atmosphere.

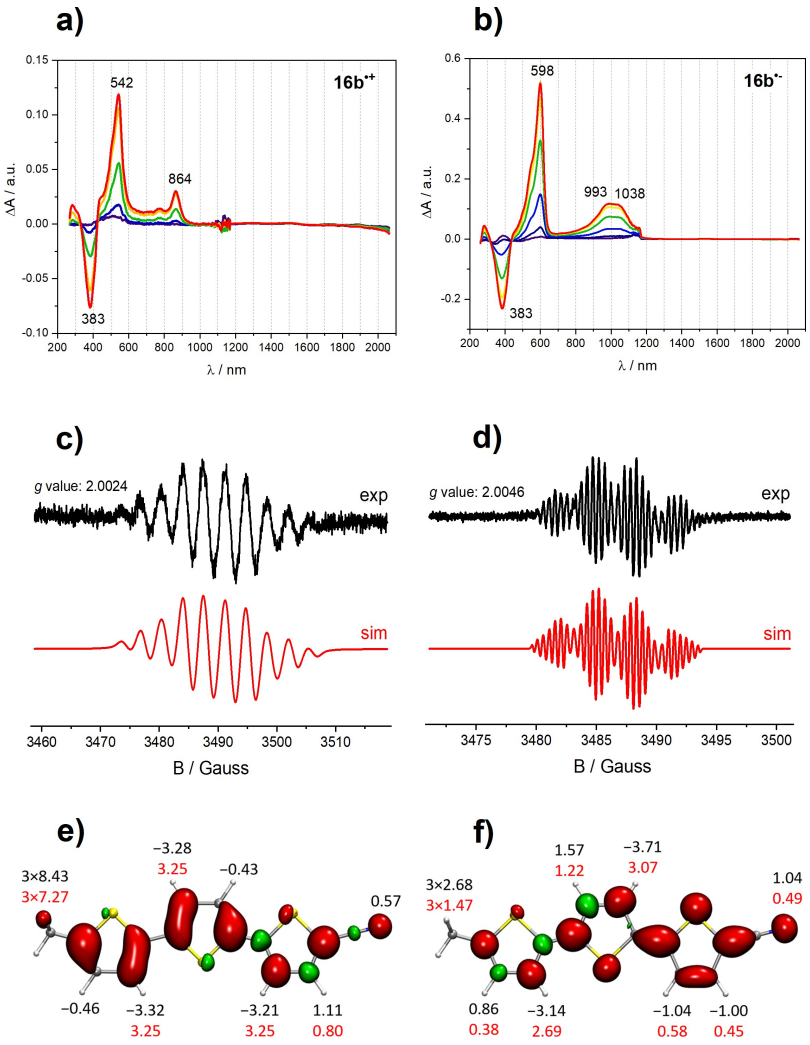

Figure 4. a,b) *In situ* UV-Vis-NIR spectra measured during the oxidation and reduction of **16b**. The negative and positive potential values increase from blue to red. c,d) Experimental and simulated EPR spectrum of the radical cation **16b**$^{\bullet+}$ and anion **16b**$^{\bullet-}$. e,f) Spin density distribution in the radical cation and anion. The numbers are hyperfine coupling constants (in Gauss) determined from the DFT calculations (black) and from the fit to the experimental EPR spectrum (red).

Density functional theory calculations

Molecular structures of neutral compounds and ions were optimized at the B3LYP–D3BJ/def2-TZVPP level in acetonitrile, electrostatic solvent correction was included with CPCM polarized continuum model. In computations of hyperfine coupling constants, EPR-III basis was used for nitrogen and hydrogen atoms. All calculations were performed with Orca suite[23] and visualized with VMD.[24]

Conclusions

Novel 2,5-bis(het)aryl substituted thiophenes have been synthesized in satisfactory yields by means of a known heterocyclization method avoiding the use of heavy metals as catalyst. The compounds exhibit a substituent-depending absorption and fluorescence in the visible region as well as adjustable redox properties. The EPR spectroelectrochemical study on selected cyano-substituted thiophenes confirms the formation of stable radical ions. The spin densities in a radical are delocalized over the whole molecule, however, it is shifted to one or another side of the molecule depending on the end-capped substituents. In the case of the 2,5-bis-thienyl substituted thiophenes, the sulfur atoms are differently involved in the spin density distribution in the radical cation and anion. The charged species of the compounds under study demonstrate strong absorptions in visible spectral region that makes them attractive as materials for electrochromic devices.[25] The redox properties of the 2,5-bis(het)aryl substituted thiophenes as well as the optical properties of the charged molecules can be tuned using appropriate substituents and/or by introduction the thiophene rings into molecular structure.

Supporting Information

The supporting information includes details of the characterization of 2,5-bis(het)aryl substituted thiophenes (yield, melting

points, ^{1}H NMR data), cyclic voltammograms, spin density distribution in radical ions as well as *in situ* UV-Vis-NIR spectra.

Acknowledgements

E.D. gratefully acknowledges financial support by the Deutsche Forschungsgemeinschaft (DFG) – DM 6/6-1. The authors thank Sandra Schiemenz (IFW Dresden) for the measurements of the UV-Vis absorption spectra.

Conflict of Interests

The authors declare no conflicts of interest.

Data Availability Statement

The data that support the findings of this study are available from the corresponding author upon reasonable request.

Keywords: density functional calculations · electron paramagnetic resonance spectroscopy · radical ions · spectroelectrochemistry · substituted thiophenes

[1] a) H. Sirringhaus, *Adv. Mater.* **2014**, *26*, 1319–1335; b) L. Zhang, N. S. Colella, B. P. Cherniawski, S. C. B. Mannsfield, A. L. Briseno, *ACS Appl. Mater. Interfaces* **2014**, *6*, 5327–5343; c) V. V. Bruevich, A. V. Glushkova, O. Yu. Pojmonova, R. S. Fedorenko, Y. N. Luponosov, A. V. Bakirov, M. A. Shcherbina, S. N. Chvalun, A. Yu. Sodsorev, L. Grodd, S. Grigorian, S. A. Ponomarenko, D. Yu. Parachuk, *ACS Appl. Mater. Interfaces* **2019**, *11*, 6315–6324.
[2] K. Walzer, B. Männig, M. Pfeiffer, K. Leo, *Chem. Rev.* **2007**, *107*, 1233–1271.
[3] J. Heeger, *Adv. Mater.* **2014**, *26*, 10–28.
[4] R. C. So, A. C. Carreon-Asok, *Chem. Rev.* **2019**, *119*, 11442–11509.
[5] S. A. Lee, Y. Yoshida, M. Fukuyama, S. Hotta, *Synth. Met.* **1999**, *106*, 39–44.
[6] S. Naqvi, N. Chaudhary, S. Singhal, P. Yadav, A. Patra, *ChemistrySelect* **2021**, *6*, 131–139.
[7] J. J. Apperloo, L. Groenendaal, H. Verheyen, M. Jayakannan, R. A. J. Janssen, A. Dkhissi, D. Beljonne, R. Lazzaroni, J.-L. Bredas, *Chem. Eur. J.* **2002**, *8*, 2384–2396.
[8] a) T. Nicolini, A. V. Marquez, B. Goudeau, A. Kuhn, G. Salinas, *J. Phys. Chem. Lett.* **2021**, *12*, 10422–10428; b) I. Bargigia, L. R. Savagian, A. M. Österholm, J. R. Reynolds, C. Silva, *J. Am. Chem. Soc.* **2021**, *143*, 294–308.
[9] a) K. Ueda, S. Yanagisawa, J. Yamaguchi, K. Itami, *Angew. Chem. Int. Ed.* **2010**, *49*, 8946–8949; b) D. Urselmann, D. Antovic, T. J. J. Mueller, *Beilstein J. Org. Chem.* **2011**, *7*, 1499–1503; c) T. Okazawa, T. Satoh, M. Miura, M. Nomura, *J. Am. Chem. Soc.* **2002**, *124*, 5286–5287; d) J. Song, F. Wei, W. Sun, X. Cao, C. Liu, L. Xie, W. Huang, *Org. Chem. Front.* **2014**, *1*, 817–820; e) M. West, A. J. B. Watson, *Org. Biomol. Chem.* **2019**, *17*, 5055–5059; f) A. Baran, M. Babkova, J. Petkus, K. Shubin, *Appl. Organomet. Chem.* **2022**, *36*, e6653; g) J. Mao, R. Li, Y. He, X. Yang, D. Wang, Y. Zhang, *Russ. J. Appl. Chem.* **2016**, *89*, 663–669; h) S. M. Spinella, Z.-H. Guan, J. Chen, X. Zhang, *Synthesis* **2009**, *18*, 3094–3098.
[10] a) M. E. Khalifa, *Synth. Comm. Rev.* **2020**, *50*, 2590–2616; b) E. R. Biehl, *Top. Heterocycl. Chem.* **2012**, *29*, 347–380; c) E. R. Biehl, *Prog. Heterocycl. Chem.* **2011**, *23*, 127–154; d) J. Schatz, *Science of Synthesis, Vol. 9,2; Hetarenes and related ring systems*, G. Thieme, Stuttgart, **2001**.
[11] J. Liebscher, H. Hartmann, *Z. Chem.* **1972**, *12*, 417–418.
[12] J. Liebscher, H. Hartmann, *Synthesis* **1979**, 241–264.
[13] a) J. Liebscher, H. Hartmann, *J. Prakt. Chem.* **1976**, *318*, 731–746; b) G. Kirsch, D. Prim, F. Leising, G. Mignani, *J. Heterocycl. Chem.* **1994**, *31*, 1005–1009.
[14] K. Bogdanowicz-Szwed, A. Budzowski, *Monatsh. Chem.* **2001**, *132*, 947–957.
[15] H.-N. Jang, H. J. No, J.-Y. Lee, B. K. Rhee, K.-H. Cho, H.-D. Cho, *Dyes Pigm.* **2009**, *82*, 209–215.
[16] J. Heinze, H. John, M. Dietrich, P. Tschuncky, *Synth. Met.* **2001**, *119*, 49–52.
[17] M. Grzybowski, B. Sadowski, H. Butenschön, D. T. Gryko, *Angew. Chem. Int. Ed.* **2020**, *59*, 2998–3027.
[18] H. Eickhoff, G. Jung, A. Rieker, *Tetrahedron* **2001**, *57*, 353–364.
[19] S. Klod, K. Haubner, E. Jähne, L. Dunsch, *Chem. Sci.* **2010**, *1*, 743–750.
[20] a) M. B. Camarada, P. Jaque, F. R. Díaz, M. A. del Valle, *J. Polym. Sci. Part B.* **2011**, *49*, 1723–1733; b) F. Pandolfi, M. Bortolami, M. Feroci, L. Mattiello, V. Scarano, D. Rocco, *Curr. Org. Chem.* **2021**, *25*, 2028–2036.
[21] C. F. R. A. C. Lima, J. C. S. Costa, A. M. S. Silva, A. Mendes, L. M. N. B. F. Santos, *J. Chem. Eng. Data* **2022**, *67*, 3033–3045.
[22] A. Neudeck, A. Petr, L. Dunsch, *Synth. Met.* **1999**, *107*, 143–158.
[23] F. Neese, *WIREs Comput. Mol. Sci.* **2018**, *8*, e1327.
[24] W. Humphrey, A. Dalke, K. Schulten, *J. Mol. Graphics* **1996**, *14*, 33–38.
[25] a) G. Cai, J. Wang, P. S. Lee, *Acc. Chem. Res.* **2016**, *49*, 1469–1476; b) C. G. Granqvist, *J. Eur. Ceram. Soc.* **2005**, *25*, 2907–2912; c) C. L. Lambert, A. Agrawal, C. Baertlien, J. Nagai, *Sol. Energy Mater. Sol. Cells* **1999**, *56*, 449–463.

Manuscript received: January 17, 2024
Revised manuscript received: January 31, 2024
Version of record online: February 21, 2024